Received: 22 July 2021 | Revised: 16 November 2021 | Accepted: 1 January 2022

DOI: 10.1111/apha.13756

ACTA PHYSIOLOGICA

GASTROINTESTINAL PHYSIOLOGY

# Enhanced phosphate absorption in intestinal epithelial cell-specific NHE3 knockout mice

**Jianxiang Xue**[1] | **Linto Thomas**[1] | **Sathish Kumar Murali**[2] | **Moshe Levi**[3] | **Robert A. Fenton**[2] | **Jessica A. Dominguez Rieg**[1,4] | **Timo Rieg**[1,4]

[1]Department of Molecular Pharmacology and Physiology, Morsani College of Medicine, University of South Florida, Tampa, Florida, USA

[2]Department of Biomedicine, Aarhus University, Aarhus, Denmark

[3]Department of Biochemistry and Molecular & Cellular Biology, Georgetown University, Washington, District of Columbia, USA

[4]James A. Haley Veterans' Hospital, Tampa, Florida, USA

**Correspondence**
Timo Rieg, Department of Molecular Pharmacology and Physiology, Morsani College of Medicine, University of South Florida, 12901 Bruce B. Downs Blvd, MDC08, Tampa, FL 33612, USA.
Email: trieg@usf.edu

**Funding information**
National Institute of Diabetes and Digestive and Kidney Diseases, Grant/Award Number: 1R01DK110621, DK076169 and DK115255; American Heart Association, Grant/Award Number: 18PRE33990236, 19POST34400026, 19TPA34850116 and 828731; Department of Veterans Affairs, Grant/Award Number: IBX004968A; Novo Nordisk Fonden, Grant/Award Number: NNF17OC0028812 and NNF19OC0058439; Det Frie Forskningsråd, Grant/Award Number: 0134-00018B

## Abstract

**Aims:** The kidneys play a major role in maintaining $P_i$ homeostasis. Patients in later stages of CKD develop hyperphosphatemia. One novel treatment option is tenapanor, an intestinal-specific NHE3 inhibitor. To gain mechanistic insight into the role of intestinal NHE3 in $P_i$ homeostasis, we studied tamoxifen-inducible intestinal epithelial cell-specific NHE3 knockout ($NHE3^{IEC\text{-}KO}$) mice.

**Methods:** Mice underwent dietary $P_i$ challenges, and hormones as well as urinary/plasma $P_i$ were determined. Intestinal $^{33}P$ uptake studies were conducted in vivo to compare the effects of tenapanor and $NHE3^{IEC\text{-}KO}$. Ex vivo $P_i$ transport was measured in everted gut sacs and brush border membrane vesicles. Intestinal and renal protein expression of $P_i$ transporters were determined.

**Results:** On the control diet, $NHE3^{IEC\text{-}KO}$ mice had similar $P_i$ homeostasis, but a ~25% reduction in FGF23 compared with control mice. Everted gut sacs and brush border membrane vesicles showed enhanced $P_i$ uptake associated with increased Npt2b expression in $NHE3^{IEC\text{-}KO}$ mice. Acute oral $P_i$ loading resulted in higher plasma $P_i$ in $NHE3^{IEC\text{-}KO}$ mice. Tenapanor inhibited intestinal $^{33}P$ uptake acutely but then led to hyper-absorption at later time points compared to vehicle. In response to high dietary $P_i$, plasma $P_i$ and FGF23 increased to higher levels in $NHE3^{IEC\text{-}KO}$ mice which was associated with greater Npt2b expression. Reduced renal Npt2c and a trend for reduced Npt2a expression were unable to correct for higher plasma $P_i$.

**Conclusion:** Intestinal NHE3 has a significant contribution to $P_i$ homeostasis. In contrast to effects described for tenapanor on $P_i$ homeostasis, $NHE3^{IEC\text{-}KO}$ mice show enhanced, rather than reduced, intestinal $P_i$ uptake.

**KEYWORDS**
chronic kidney disease, homeostasis, inhibitor, intestine, phosphate, sodium-hydrogen exchanger 3

Jianxiang Xue and Linto Thomas contributed equally to this work.

## 1 | INTRODUCTION

The $Na^+/H^+$ exchanger isoform 3 (NHE3) mediates $Na^+$ (re)uptake in the intestine and kidneys.[1,2] In the intestine, the $Na^+$ transport by NHE3 is critical for fluid absorption, and inducible knockout of NHE3 selectively in the small intestine and colon ($NHE3^{IEC\text{-}KO}$) results in persistent diarrhoea, increased mortality rate, metabolic acidosis, lower blood bicarbonate levels, hyponatremia and hyperkalaemia associated with drastically elevated plasma aldosterone levels and changes to intestinal structural integrity.[3] Most of these pathologies are similar to patients suffering from congenital $Na^+$ diarrhoea[4] and some are consistent with whole-body NHE3 knockout mice.[2,5]

In recent years, intestinal NHE3 has become a pharmacological target. The development of tenapanor (AZD1722, RDX5791), an inhibitor of NHE3 that is minimally absorbed from the gastrointestinal tract, is approved by the FDA for treatment of irritable bowel syndrome with constipation.[6] Consistent with data from $NHE3^{IEC\text{-}KO}$ mice, humans treated with tenapanor display increased stool frequency, reduced stool consistency and increased faecal $Na^+$[7,8] alongside decreased urinary $Na^+$ excretion,[7] the latter possibly as a consequence of the activation of the renin-angiotensin-aldosterone system. Diarrhoea was the most frequently observed side effect. In addition to this, tenapanor alters $P_i$ homeostasis by potentially reducing intestinal paracellular $P_i$ transport and via a reduced expression of the intestinal $Na^+$-$P_i$ cotransporter 2b (Npt2b).[9] In clinical studies, tenapanor can reduce plasma $P_i$ in patients on haemodialysis with hyperphosphatemia treated with[10] or without[11] $P_i$ binders. This was accompanied by reduced fibroblast growth factor 23 (FGF23),[12] a major hormone contributing to the development of left ventricular hypertrophy in chronic kidney disease (CKD).[13] Based on these findings, the use of tenapanor for the control of plasma $P_i$ in adult patients with CKD on dialysis has been requested for US regulatory approval but was recently denied because of a "small" effect.[14]

The aim of the current study was to use a mouse model with an inducible knockout of NHE3 in intestinal epithelial cells to assess the role of intestinal NHE3 in $P_i$ homeostasis and whether genetic deletion of NHE3 in mice mimics observations using tenapanor in humans. We hypothesized that, based on experiments with tenapanor,[9,15] $NHE3^{IEC\text{-}KO}$ mice will show reduced $P_i$ absorption from the intestine, elevated intestinal content $P_i$ levels and consequently, reduced plasma $P_i$, PTH and FGF23 levels alongside increased renal $P_i$ transporter expression. Further studies are warranted to understand the mechanistic differences between intestinal-specific NHE3 inhibitors and $NHE3^{IEC\text{-}KO}$ mice.

## 2 | RESULTS

### 2.1 | Baseline $P_i$ phenotype in $NHE3^{IEC\text{-}KO}$ mice

Body weight was not significantly different between control and tamoxifen-induced $NHE3^{IEC\text{-}KO}$ mice 2 weeks after tamoxifen administration on the control $P_i$ diet (Figure 1A). Measurements of fluid and food intake in their home cages showed that $NHE3^{IEC\text{-}KO}$ mice had a ~1.2-fold greater food intake (Figure 1B) in combination with a ~1.8-fold greater fluid intake (Figure 1C) compared with control mice. Blood and urine analysis showed no significant differences in plasma $P_i$ concentrations (Figure 1D) and urinary creatinine/$P_i$ ratio (Figure 1E) between genotypes. In contrast to plasma parathyroid hormone (PTH) levels, which were similar between genotypes (Figure 1F), FGF23 levels were ~25% reduced in $NHE3^{IEC\text{-}KO}$ compared with the control mice (Figure 1G). In a different cohort of mice on the control $P_i$ diet, intestinal content was analysed 2 weeks after tamoxifen administration. Intestinal content (proximal and distal small intestine as well as the colon) was greater in all regions of the intestine (Figure 1H), with the combined total intestinal content ~2-fold greater in $NHE3^{IEC\text{-}KO}$ compared with the control mice ($1.2 \pm 0.1$ vs $0.5 \pm 0.1$ g, $P < .05$). Similarly, intestinal $Na^+$ content was greater in all regions (Figure 1I), leading to an ~3-fold greater total intestinal $Na^+$ content in $NHE3^{IEC\text{-}KO}$ compared with the control mice ($126 \pm 6$ vs $41 \pm 3$ μmol, $P < .05$; Figure 1I). In contrast, intestinal $P_i$ content in the proximal and distal small intestine was not significantly different between genotypes (Figure 1J). $P_i$ content in the colon was ~1.9-fold greater in $NHE3^{IEC\text{-}KO}$ compared with control mice (Figure 1J), which was also reflected in total intestinal $P_i$ amounts being slightly (~1.3-fold) greater in $NHE3^{IEC\text{-}KO}$ compared with the control mice ($24 \pm 2$ vs $18 \pm 2$ μmol, $P < .05$).

### 2.2 | Intestinal $P_i$ transport in $NHE3^{IEC\text{-}KO}$ mice on the control diet

Mice were studied on the control $P_i$ diet 2 weeks after tamoxifen administration. In everted gut sac experiments no differences in $Na^+$-dependent $P_i$ uptake were observed in the duodenum between genotypes (Figure 2A). $Na^+$-dependent $P_i$ uptake in the jejunum was significantly greater in $NHE3^{IEC\text{-}KO}$ mice relative to controls, whereas in the ileum, it was significantly less (Figure 2A). This suggests that the overall $P_i$ uptake in the absence of NHE3 increases in the proximal parts of the intestine but decreases in the distal portions. $Na^+$-independent uptake (measured by replacing $Na^+$ with choline $Cl^-$) was not significantly

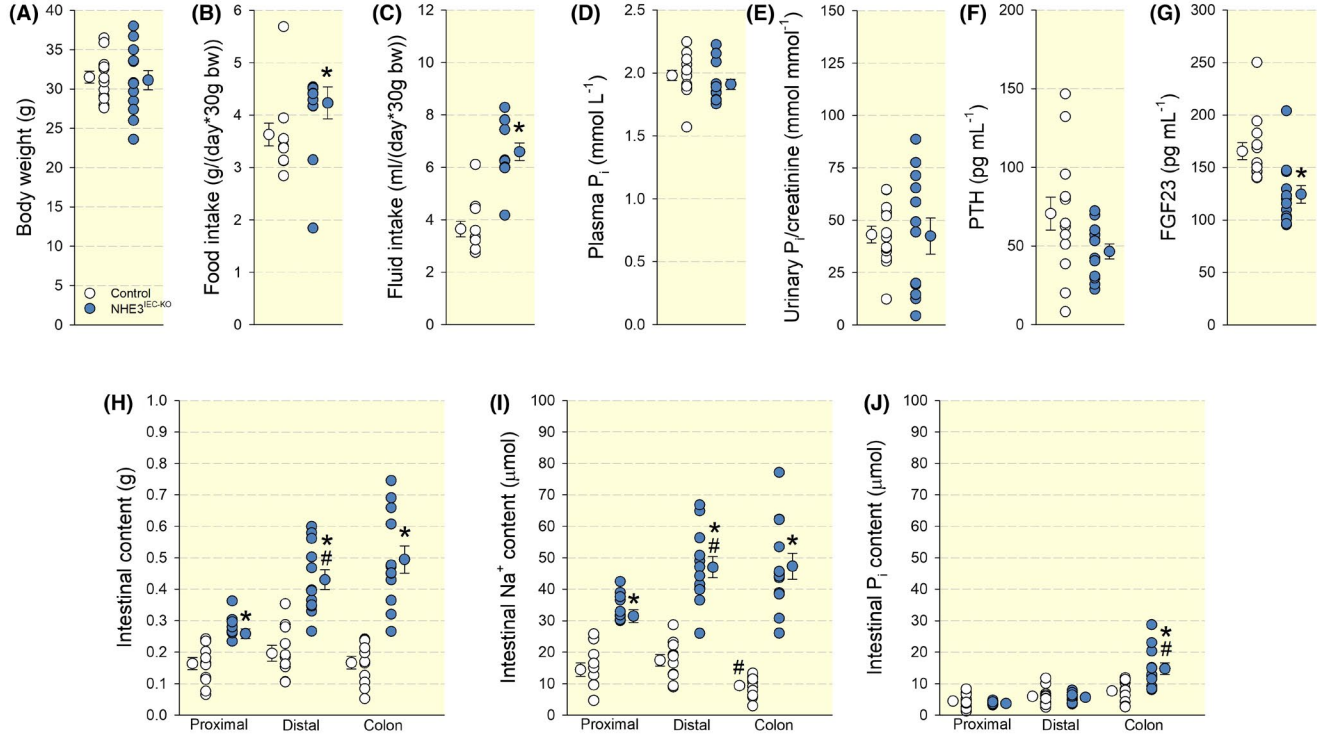


**FIGURE 1** Intestinal knockout of NHE3 results in lower plasma FGF23 and enhanced $P_i$ content in the colon. Physiological analysis of control and NHE3$^{IEC\text{-}KO}$ mice 2 weeks after tamoxifen administration on control diet (n = 11-12/genotype). (A) Body weight, (B) food and (C) fluid intake were averaged over the 2-week period. (D) Plasma $P_i$, (E) urinary $P_i$/creatinine and (F) PTH were not different between genotypes. In contrast, (G) FGF23 was significantly lower in NHE3$^{IEC\text{-}KO}$ compared with the control mice. In a different cohort of mice, intestinal content was analysed 2 weeks after tamoxifen administration (n = 11-12/genotype). Amounts of (H) content and (I) $Na^+$ in each segment were significantly greater in NHE3$^{IEC\text{-}KO}$ compared with the control mice. In contrast, the amount of (J) $P_i$ was slightly but significantly greater only in the colon of NHE3$^{IEC\text{-}KO}$ mice. Male mice were used in these studies. Data are expressed as mean ± SEM and were analysed by Student's *t* test (A-G) and repeated measures mixed-effects model followed by Tukey's multiple comparisons test (H-J). $^*P < .05$ vs control, $^{\#}P < .05$ vs previous intestinal segment in the same genotype

different from zero in all segments or between genotypes (Figure S1A). Glucose uptake was greater in jejunum and ileum relative to the duodenum in both genotypes, but glucose uptake was not significantly different between genotypes in all studied segments (Figure 2B).

To further study $P_i$ transport across the apical membrane, brush border membrane vesicles (BBMV) from each intestinal region were isolated. In control mice, $Na^+$-dependent $^{32}P$ uptake in BBMV was lowest in the duodenum (Figure 2C) and jejunum (Figure 2D) and significantly greater in the ileum (Figure 2E). In $Na^+$-free conditions (balanced using choline $Cl^-$) or a non-specific Npt2 inhibitor (phosphonoformic acid, PFA), $^{32}P$ uptake in control mice was low in all intestinal regions (Figure 2C-E). In contrast, $Na^+$-dependent $^{32}P$ uptake in NHE3$^{IEC\text{-}KO}$ mice was lowest in the duodenum (Figure 2C) but significantly greater in the jejunum (~5-fold higher than in control mice; Figure 2D) and ileum (Figure 2E). In $Na^+$-free conditions or the presence of PFA, $^{32}P$ uptake in NHE3$^{IEC\text{-}KO}$ mice was significantly reduced to levels seen in control mice (Figure 2C-E). Intestinal Npt2b protein expression in acutely isolated intestinal epithelial cells was ~2-fold greater in NHE3$^{IEC\text{-}KO}$ compared with the control mice (Figure 2F). Claudin-3, a paracellular barrier-forming tight junction protein involved in $P_i$ transport,[16] was not significantly different between genotypes (Figure S1B). To assess the ability of NHE3$^{IEC\text{-}KO}$ mice to respond to an acute oral $P_i$ load 1 week after tamoxifen administration, mice were given 0.5 mol $L^{-1}$ $NaH_2HPO_4$ and plasma $P_i$ levels were assessed. Before the gavage of $NaH_2PO_4$, plasma $P_i$ levels were not significantly different between genotypes (Figure 2G). One hour after gavage, plasma $P_i$ levels increased to a significantly greater extent in NHE3$^{IEC\text{-}KO}$ compared to the control mice (2.0 ± 0.2 vs 1.1 ± 0.1 mmol $L^{-1}$, $P < .05$; Figure 2G). To compare the $P_i$ uptake in NHE3$^{IEC\text{-}KO}$ mice and pharmacological inhibition of intestinal NHE3, the appearance of $^{33}P$ in plasma was studied following administration of either vehicle or tenapanor. In control mice, intestinal $^{33}P$ uptake was ~67% lower in response to tenapanor treatment after 5 minutes compared with vehicle-treated control mice (Figure 3A). However, at later time points, tenapanor-treated control

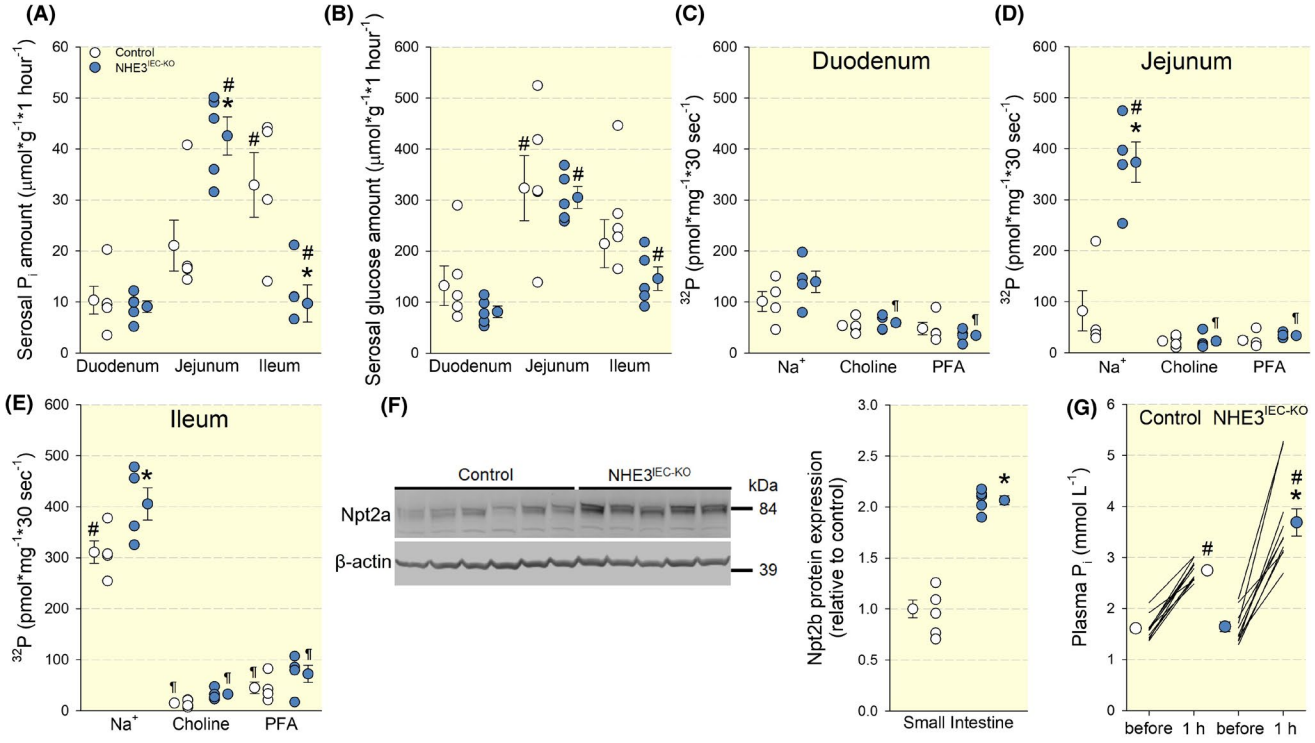


**FIGURE 2** Intestinal knockout of NHE3 alters $P_i$ transport on the control diet. Everted gut sac experiments of control and NHE3$^{IEC-KO}$ mice 2 weeks after tamoxifen administration on control diet (n = 4-5/genotype). Serosal (A) $P_i$ amount and serosal (B) glucose amount in duodenum, jejunum and ileum. In another cohort, transport studies in acutely isolated brush border membrane vesicles were performed in (C) duodenum, (D) jejunum and (E) ileum in the presence of $Na^+$, choline $Cl^-$ ($Na^+$-independent) or PFA (Npt2b-dependent) (n = 8/genotype, tissues from 2 mice were pooled). (F) In another cohort, Npt2b expression (predicted molecular weight ~76 kDa; β-actin, predicted molecular weight ~42 kDa) was determined in intestinal epithelial cells of the small intestine. Intestinal epithelial cells were isolated 2 weeks after tamoxifen administration on the control diet (n = 5-6/genotype). (G) Plasma $P_i$ before and 1 hour after an acute oral $P_i$ load (0.5 mol $L^{-1}$ $NaH_2HPO_4$ via oral gavage) (n = 10-11/genotype). Male mice were used in all studies except for BBMV, where female mice were used. Data are expressed as mean ± SEM. Data were analysed by repeated measures mixed-effects model followed by Šidák multiple comparisons test (A, B), repeated-measures two-way ANOVA followed by Šidák multiple comparisons test (C-E and G) and Student's *t* test (F). *$P < .05$ vs control, $^{\#}P < .05$ vs previous segment/before $P_i$ load same genotype. $^{¶}P < .05$ vs $Na^+$-dependent transport same genotype

mice showed an increase in intestinal $P_i$ uptake, reaching a maximum of $^{33}P$ in plasma after 60 minutes; this contrasts with vehicle-treated control mice who showed a continuous decline in $^{33}P$ uptake after 30 minutes. In NHE3$^{IEC-KO}$ mice, tenapanor and vehicle administration showed a similar pattern of $^{33}P$ uptake (Figure 3B); however, as seen in the tenapanor-treated control mice, tenapanor-treated NHE3$^{IEC-KO}$ mice reached a maximum of $^{33}P$ in plasma after 60 minutes. Vehicle administration to control and NHE3$^{IEC-KO}$ mice only showed a difference in $P_i$ uptake at the 5-minute time point (Figure 3C). Control and NHE3$^{IEC-KO}$ mice showed a similar pattern in response to tenapanor administration; however, there is a clear distinction in the magnitude of the effect and at the 60-minute time point, plasma $^{33}P$ was significantly lower in tenapanor-treated NHE3$^{IEC-KO}$ compared with tenapanor-treated control mice (Figure 3D). No differences in the area under the curve were observed between genotypes or treatment (Figure 3E).

## 2.3 | Effects of high dietary $P_i$ intake

Average body weight and food intake on a a high $P_i$ diet were not significantly different between genotypes (Figure 4A,B). Fluid intake was ~2-fold greater in NHE3$^{IEC-KO}$ compared with control mice (Figure 4C). The intestinal content after 2 weeks on high $P_i$ diet was greater in the proximal and distal segments in NHE3$^{IEC-KO}$ compared with control mice, but not in the colon (Figure 4D), resulting in an ~3-fold greater total intestinal content in NHE3$^{IEC-KO}$ mice (0.8 ± 0.1 vs 0.3 ± 0.1 g, $P < .05$). Compared to the control diet, the total intestinal content on the high $P_i$ diet tended to be lower possibly because of a trend for lower food intake. Total intestinal $Na^+$ content was ~2.5-fold greater in NHE3$^{IEC-KO}$ mice compared with control mice (64 ± 5 vs 25 ± 4 µmol, $P < .05$; Figure 4E), predominantly because of enhanced $Na^+$ content in the proximal and distal segments. In contrast, intestinal $P_i$ content in the proximal and distal small intestine as well as

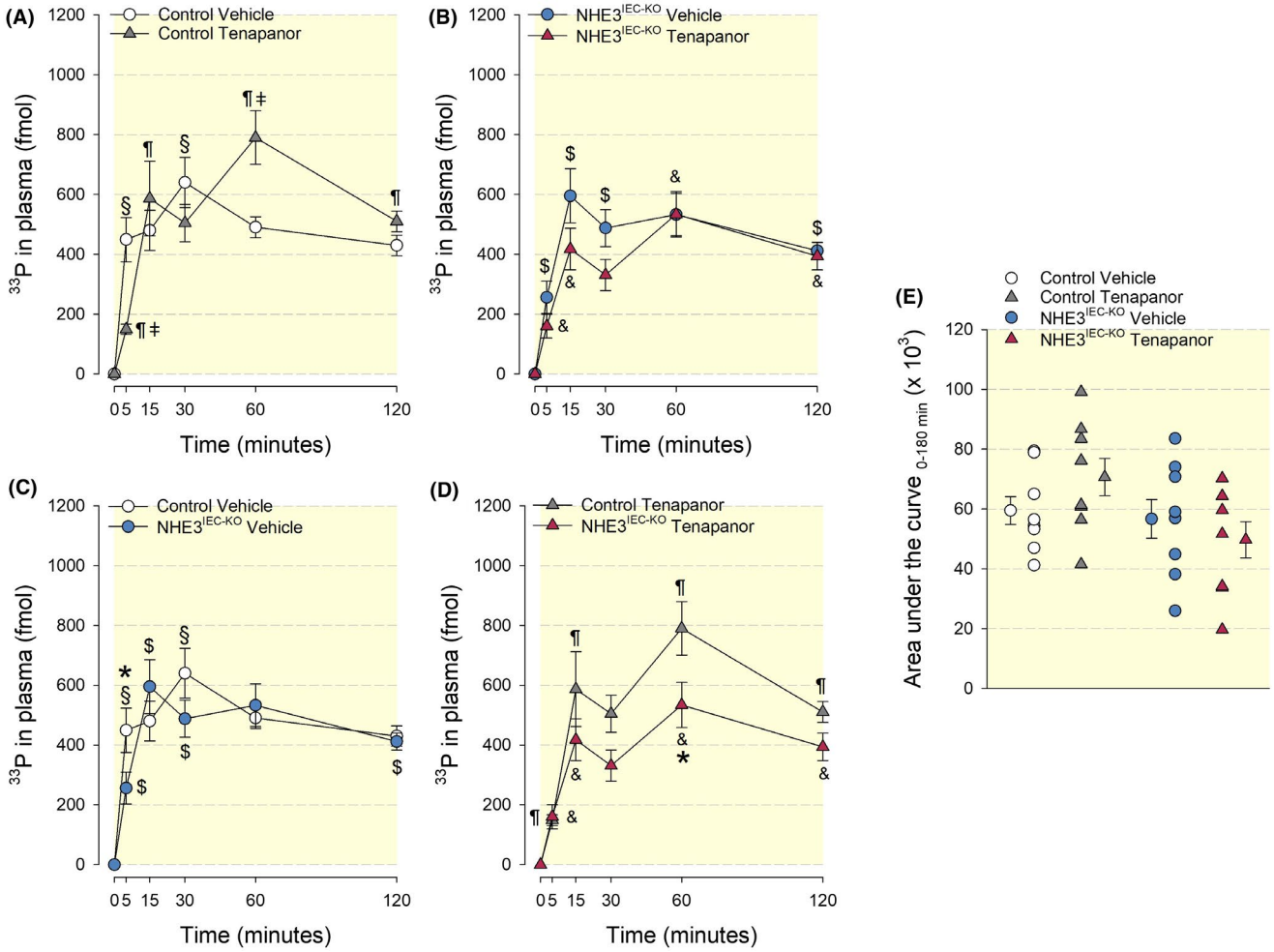


**FIGURE 3** Tenapanor inhibits intestinal $^{33}$P uptake in vivo only at the 5-minute time point. Oral co-administration (after overnight fasting) of vehicle or tenapanor (30 mg kg$^{-1}$) with $^{33}$P in control and NHE3$^{IEC-KO}$ mice 2 weeks after tamoxifen administration on control diet (n = 8/genotype and treatment). Effect of vehicle and tenapanor in (A) control and (B) NHE3$^{IEC-KO}$ mice. Comparison of (C) vehicle and (D) tenapanor effects between genotypes. (E) Corresponding area under the curve (AUC) analysis. Male mice were used in these studies. Data are expressed as mean ± SEM and were analysed by repeated-measures two-way mixed-effects model followed by a two-stage linear step-up procedure of Benjamini, Krieger and Yekutieli (A–D) and one-way ANOVA followed by Tukey's multiple comparisons test (F). *$P < .05$ vs control, $^{§}P < .05$ vs previous time point in control vehicle, $^{¶}P < .05$ vs previous time point in control tenapanor, $^{ǂ}P < .05$ vs control vehicle, $^{$}P < .05$ vs previous time point in NHE3$^{IEC-KO}$ vehicle, $^{&}P < .05$ vs previous time point in NHE3$^{IEC-KO}$ tenapanor

in the colon were not significantly different between genotypes (Figure 4F), leading to total intestinal $P_i$ amounts not being significantly different between NHE3$^{IEC-KO}$ and control mice (34 ± 7 vs 39 ± 6 μmol, $P < .05$; Figure 4F). In response to the high $P_i$ diet, total intestinal $P_i$ amounts were ~2.2 and ~1.4-fold greater in control and NHE3$^{IEC-KO}$ mice, respectively, compared with the control diet ($P < .05$).

In control mice, plasma $P_i$ (Figure 5A), PTH (Figure 5B) and FGF23 (Figure 5C) did not significantly change after tamoxifen administration. Of note, plasma $P_i$ slightly but significantly decreased (−0.25 ± 0.1 mmol L$^{-1}$, $P < .05$; Figure 5A) in response to high dietary $P_i$. This was possibly the consequence of the combination of elevated PTH (Figure 5B) and FGF23 levels (Figure 5C) in control mice fed the high $P_i$ diet. Similar to control mice, plasma $P_i$ (Figure 5A) and PTH (Figure 5B) were not significantly changed after tamoxifen administration in NHE3$^{IEC-KO}$ mice. FGF23 levels significantly decreased (−76 ± 11 pg mL$^{-1}$, $P < .05$, Figure 5C) after tamoxifen administration on the control diet in NHE3$^{IEC-KO}$ mice. In contrast to control mice, high dietary $P_i$ significantly increased plasma $P_i$ in NHE3$^{IEC-KO}$ mice (0.5 ± 0.1 mmol L$^{-1}$, $P < .05$; Figure 5A), which was associated with significantly increased plasma PTH levels (not significantly different from the control mice; Figure 5B). On a high $P_i$ diet, FGF23 levels also increased to a significantly greater extent than in the control mice (552 ± 66 vs 244 ± 14 pg mL$^{-1}$, $P < .05$; Figure 5C). Consistent with a high-dietary $P_i$ content, urinary $P_i$/creatinine ratios increased significantly in

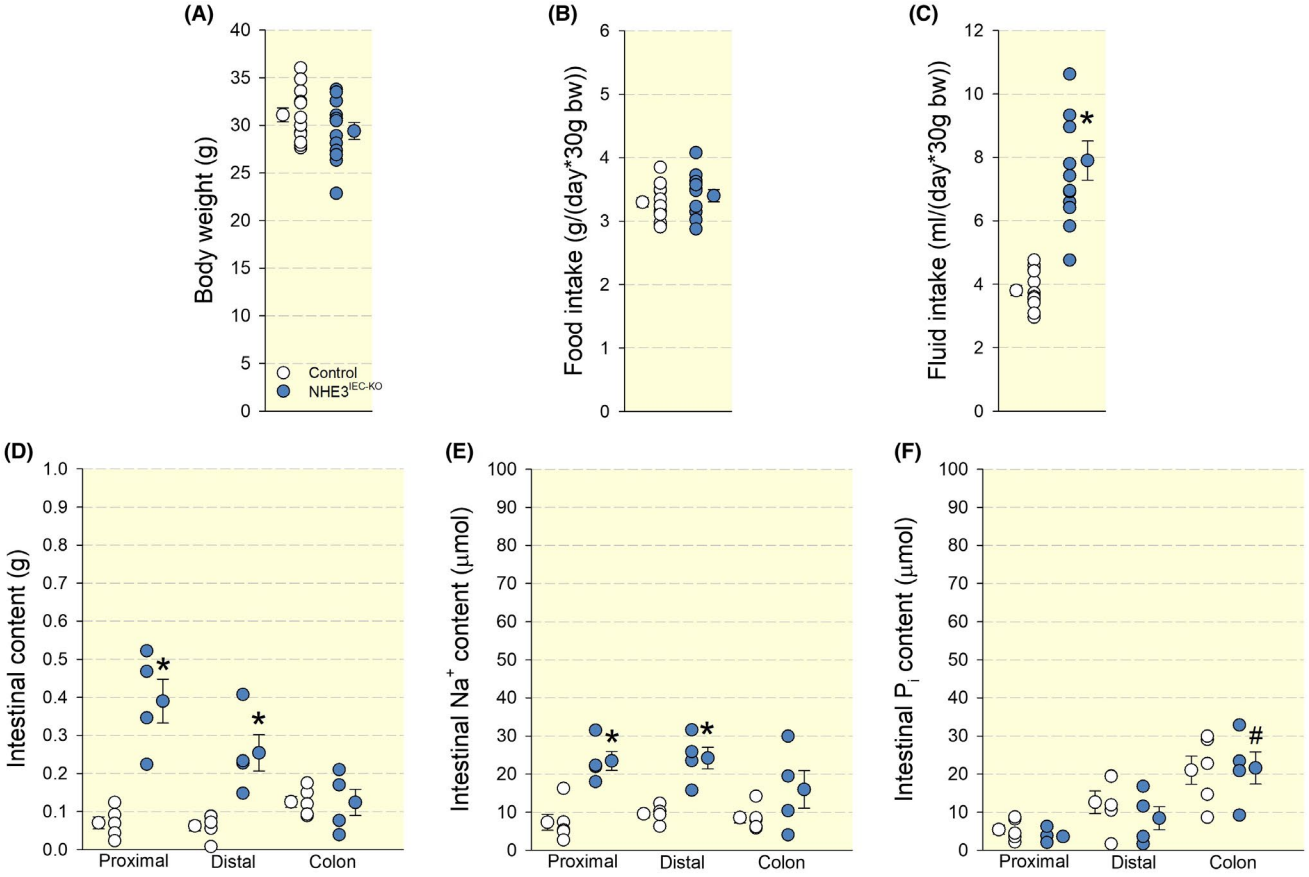


**FIGURE 4** Response to high dietary $P_i$ in control and NHE3$^{IEC-KO}$ mice. Physiological analysis of control and NHE3$^{IEC-KO}$ mice after 2 weeks on high dietary $P_i$ (n = 11-12/genotype). (A) Body weight, (B) food and (C) fluid intake was averaged over the 2-week period. After 2 weeks, intestinal contents were collected (n = 4-5/genotype). Amounts of (D) content and (E) $Na^+$ were significantly greater in the proximal and distal small intestine of NHE3$^{IEC-KO}$ compared with the control mice. In contrast, the amount of (F) $P_i$ was not significantly different between genotypes but increased significantly in the colon compared to the distal small intestine in NHE3$^{IEC-KO}$ mice. Male mice were used in these studies. Data are expressed as mean ± SEM and were analysed by Student's *t* test (A-C) and repeated measures mixed-effects model followed by Šidák multiple comparisons test (H-J). $^*P < .05$ vs control, $^{\#}P < .05$ vs previous intestinal segment in the same genotype

both genotypes; however, the urinary $P_i$/creatinine ratio was ~1.4-fold greater in NHE3$^{IEC-KO}$ compared with the control mice (Figure 5D).

On a high $P_i$ diet, intestinal Npt2b expression was significantly greater in the proximal (~2.8-fold) and distal small intestine (~1.7-fold) in NHE3$^{IEC-KO}$ compared with the control mice (Figure 6A). Renal Npt2a expression trended to be lower (~25%) and Npt2c expression was significantly lower (~50%) in NHE3$^{IEC-KO}$ compared with the control mice (Figure 6B), potentially because of the higher FGF23 levels. To assess the ability of NHE3$^{IEC-KO}$ mice to respond to an acute oral $P_i$ load under high dietary $P_i$, mice were gavaged with 0.5 mol $L^{-1}$ $NaH_2PO_3$ after 1 week on high dietary $P_i$. Before gavage, plasma $P_i$ levels were significantly greater (~0.6 mmol $L^{-1}$, $P < .05$; Figure 6C) in NHE3$^{IEC-KO}$ compared with control mice. One hour after gavage, plasma $P_i$ was significantly increased in both genotypes, but remained significantly greater in NHE3$^{IEC-KO}$ compared with the control mice (~0.4 mmol $L^{-1}$, $P < .05$; Figure 6C). However, the fold increase in plasma $P_i$ was slightly but significantly smaller in NHE3$^{IEC-KO}$ compared with the control mice (0.7 ± 0.1 vs 0.9 ± 0.1 mmol $L^{-1}$ in controls, $P < .05$; Figure 6C). To study if compensatory changes in the intestine occurred, we compared Pit1 (a high-affinity $Na^+$-dependent $P_i$ transporter) and claudin-3 expression between genotypes on a high $P_i$ diet. No significant differences were observed between Pit1 or claudin-3 expression between genotypes and intestinal segments (Figure 7A,B).

## 3 | DISCUSSION

A recent study proposes that tenapanor, an intestinal-specific NHE3 inhibitor, can reduce paracellular intestinal $P_i$ absorption thereby reducing plasma $P_i$ levels.[9] To

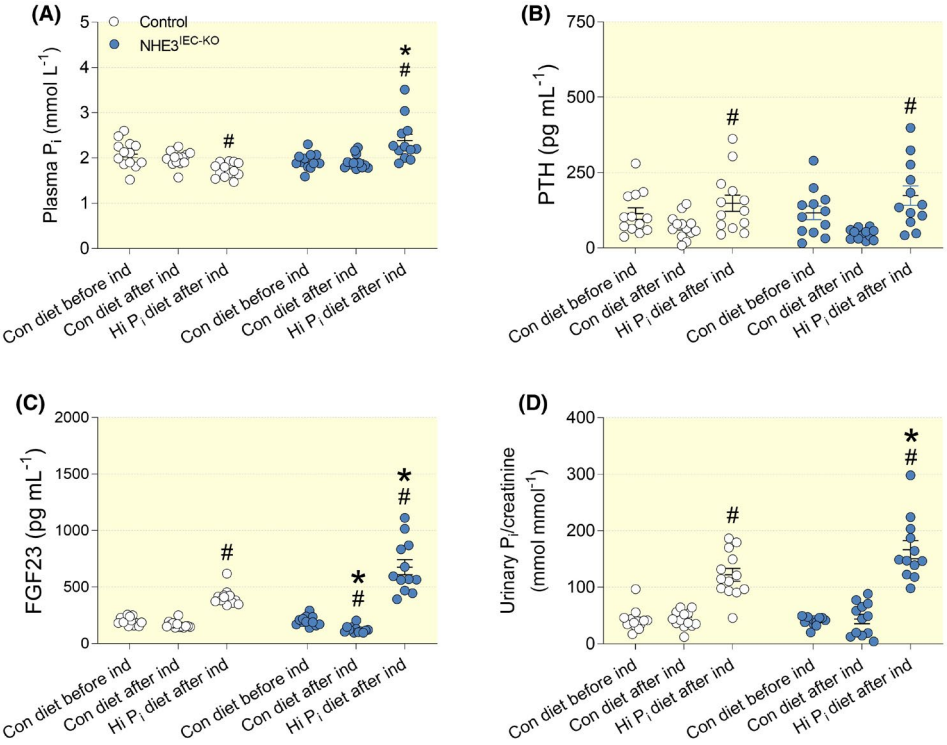


**FIGURE 5** Higher plasma $P_i$ and FGF23 levels in response to high dietary $P_i$ in NHE3$^{IEC\text{-}KO}$ mice. Physiological analysis of control and NHE3$^{IEC\text{-}KO}$ mice before tamoxifen induction on control diet (Con diet before ind), 2 weeks after tamoxifen induction on control diet (Con diet after ind) and after 2 weeks on high $P_i$ diet (Hi $P_i$ diet after ind). (A) Plasma $P_i$ decreased slightly but significantly in control mice in response to high $P_i$, a response that was the complete opposite in NHE3$^{IEC\text{-}KO}$ mice. (B) No differences in PTH responses were observed. (C) FGF23 increased to a significantly greater amount in response to high dietary $P_i$ in NHE3$^{IEC\text{-}KO}$ compared with control mice. (D) Urinary $P_i$/creatinine ratios increased in response to high dietary $P_i$; however, the increase was significantly greater in NHE3$^{IEC\text{-}KO}$ compared with control mice. Male mice were used in these studies. Data are expressed as mean ± SEM. *$P < .05$ vs control, $^{\#}P < .05$ vs previous time interval in the same genotype

gain further mechanistic insight into the role of intestinal NHE3 in $P_i$ homeostasis, we studied inducible intestinal epithelial cell-specific NHE3 knockout mice.[3] Surprisingly, our ex vivo data in everted gut sacs and BBMVs suggest a different role of intestinal NHE3 in $P_i$ homeostasis; with a lack of intestinal NHE3 enhancing, not inhibiting, intestinal $P_i$ absorption. Our in vivo studies in mice on control or high dietary $P_i$ showed that lack of intestinal NHE3 is associated with greater intestinal Npt2b expression and elevated plasma $P_i$ levels that require significantly greater FGF23 levels to increase urinary $P_i$ excretion and maintain $P_i$ balance; the latter possibly a consequence of significantly lower renal Npt2c expression.

The expression of NHE3 along the murine intestine is highest in the jejunum followed by the duodenum, with very low expression levels in the ileum.[1,17] Lack of intestinal NHE3 resulted in greater luminal $Na^+$ content from the proximal to the distal small intestine and significantly greater total luminal $Na^+$ content. This was also associated with an increased total intestinal content weight and, as we previously published for NHE3$^{IEC\text{-}KO}$ mice,[3] enhanced faecal water content. Of note, in young juvenile rats, tenapanor caused death possibly as a consequence of dehydration.[18] Our findings are consistent with other studies that have used tenapanor to pharmacologically inhibit intestinal NHE3. In rats, tenapanor inhibited intestinal $Na^+$ uptake, resulting in increased faecal $Na^+$ and the total amount of luminal content.[7] In healthy human volunteers, tenapanor also increased faecal $Na^+$ content.[7]

In addition to increased luminal $Na^+$ content, pharmacological inhibition of intestinal NHE3 with tenapanor in rats increased the luminal $P_i$ delivery in the caecum ~10-fold 2 hours after administration.[9] Since the majority of $P_i$ absorption occurs in the small intestine, the authors concluded that any luminal $P_i$ content more distally represented $P_i$ that was not absorbed.[9] However, a study in rats maintained on a normal $P_i$ diet found that the free luminal $P_i$ concentration was ~1.8-fold greater in the colon than in the small intestine.[19] Our studies in NHE3$^{IEC\text{-}KO}$ mice also showed a significantly greater luminal $P_i$ amount in the colon; however, luminal $P_i$ content in the proximal and distal small intestine was the same as in control mice. The latter contrasts with what was observed in NHE3$^{IEC\text{-}KO}$ mice for luminal $Na^+$ content, which showed a clear

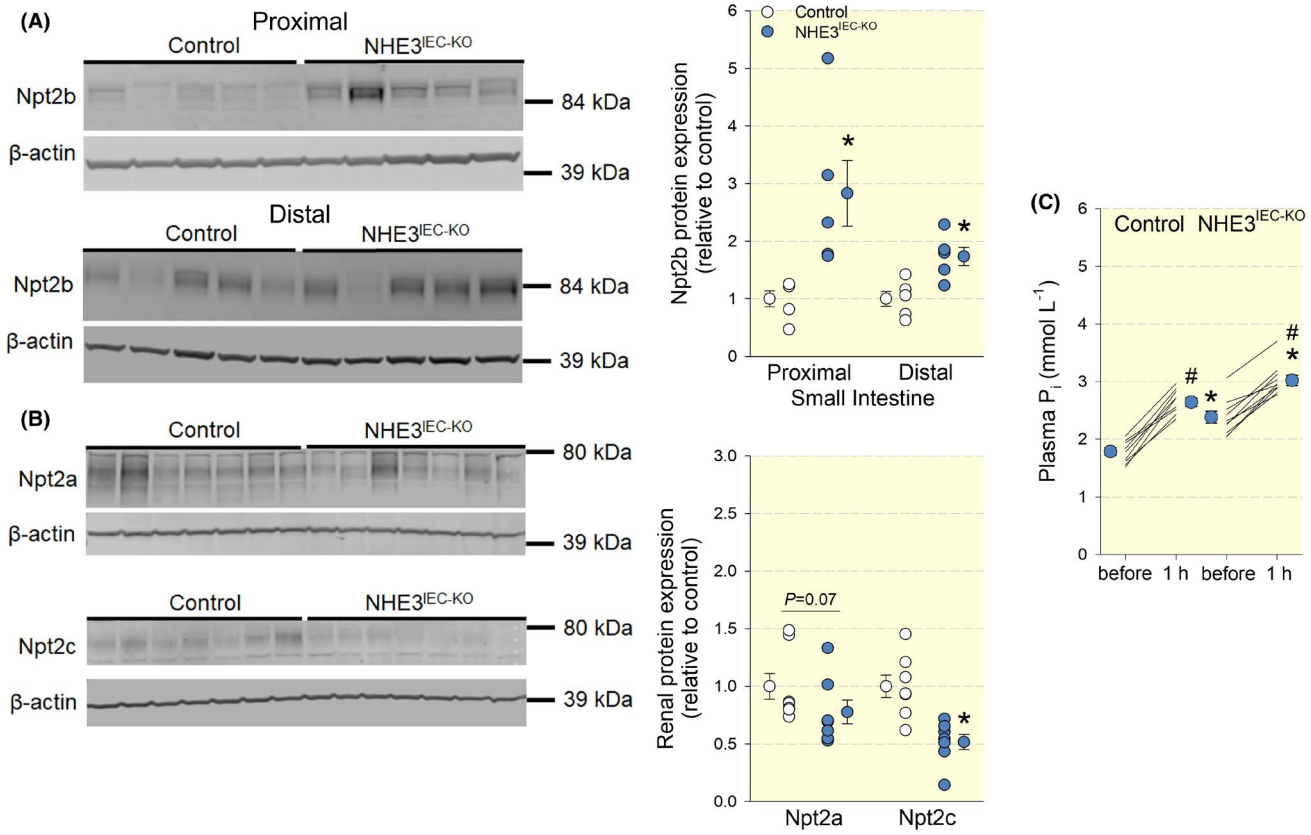


**FIGURE 6** Greater intestinal Npt2b expression associated with lower Npt2c expression on a high $P_i$ diet in NHE3$^{IEC\text{-}KO}$ mice. Intestinal epithelial cells were isolated 2 weeks after high dietary $P_i$ feeding. (A) Npt2b protein expression (predicted molecular weight ~76 kDa; β-actin, predicted molecular weight ~42 kDa) was significantly greater in NHE3$^{IEC\text{-}KO}$ compared to control mice in the proximal and distal small intestine (n = 5/genotype). (B) Npt2a protein expression (predicted molecular weight ~69 kDa) tended to be lower and Npt2c protein expression (predicted molecular weight ~64 kDa) was significantly lower in NHE3$^{IEC\text{-}KO}$ compared to control mice. (C) Plasma $P_i$ (before) was significantly higher after 1 week on high dietary $P_i$ in NHE3$^{IEC\text{-}KO}$ compared with control mice. In addition, 1 hour after an acute oral $P_i$ load (0.5 mol $L^{-1}$ $NaH_2HPO_4$ via oral gavage) plasma $P_i$ was significantly greater in NHE3$^{IEC\text{-}KO}$ (n = 10) compared with control mice (n = 10). Male mice were used in these studies. Data are expressed as mean ± SEM. Data were analysed by Student's *t* test (A, B) and repeated measures two-way ANOVA followed by Šidák multiple comparisons test (C). $^{*}P < .05$ vs control, $^{\#}P < .05$ vs before $P_i$ load same genotype

increase compared to control mice. The greater luminal $P_i$ content in the colon was seen in mice on both control and high $P_i$ diet; whether this increase is because of the inhibition of $P_i$ transport in the colon, secretion of $P_i$ in the colon,[20] or if this is even a NHE3-dependent mechanism, remains to be determined.

In the intestine, $P_i$ is absorbed via 2 distinct mechanisms: $Na^+$-dependent secondary active transport and passive paracellular transport. In mice, maximal intestinal $P_i$ absorption occurs in the ileum, correlating with the highest expression of Npt2b.[21] This is in contrast to rats and humans, which have maximal intestinal $P_i$ absorption in the duodenum.[22,23] Our studies in everted gut sacs and BBMV of control mice confirm that $P_i$ uptake is highest in the ileum of mice. Interestingly, in NHE3$^{IEC\text{-}KO}$ mice, intestinal $Na^+$-dependent $P_i$ transport was (a) greater and (b) shifted to more proximal intestinal segments. Consistent with other studies,[24] removal of $Na^+$ or PFA treatment significantly lowered $P_i$ uptake. NHE3$^{IEC\text{-}KO}$ mice on the control $P_i$ diet also exhibited greater intestinal Npt2b expression. The mechanism(s) for this greater Npt2b expression remain elusive but might relate to a compensatory response to increase intestinal $Na^+$ uptake in the absence of NHE3. A paradoxical greater Npt2b expression, $P_i$ transport and plasma $P_i$ were also observed when rats were adapted to a low $P_i$ diet and acutely challenged by high dietary $P_i$[25]; however, the mechanism(s) remain unknown. Glucose transport was consistent with the greatest Sglt1 expression in the jejunum,[26] but was not significantly different between genotypes, the former confirming the viability of the everted gut sac preparations. Acute oral $P_i$ loading, a manoeuvre that uncovered an ~50% reduction of $P_i$ uptake in Npt2b knockout mice,[27] resulted in greater plasma $P_i$ levels in NHE3$^{IEC\text{-}KO}$ mice, which is

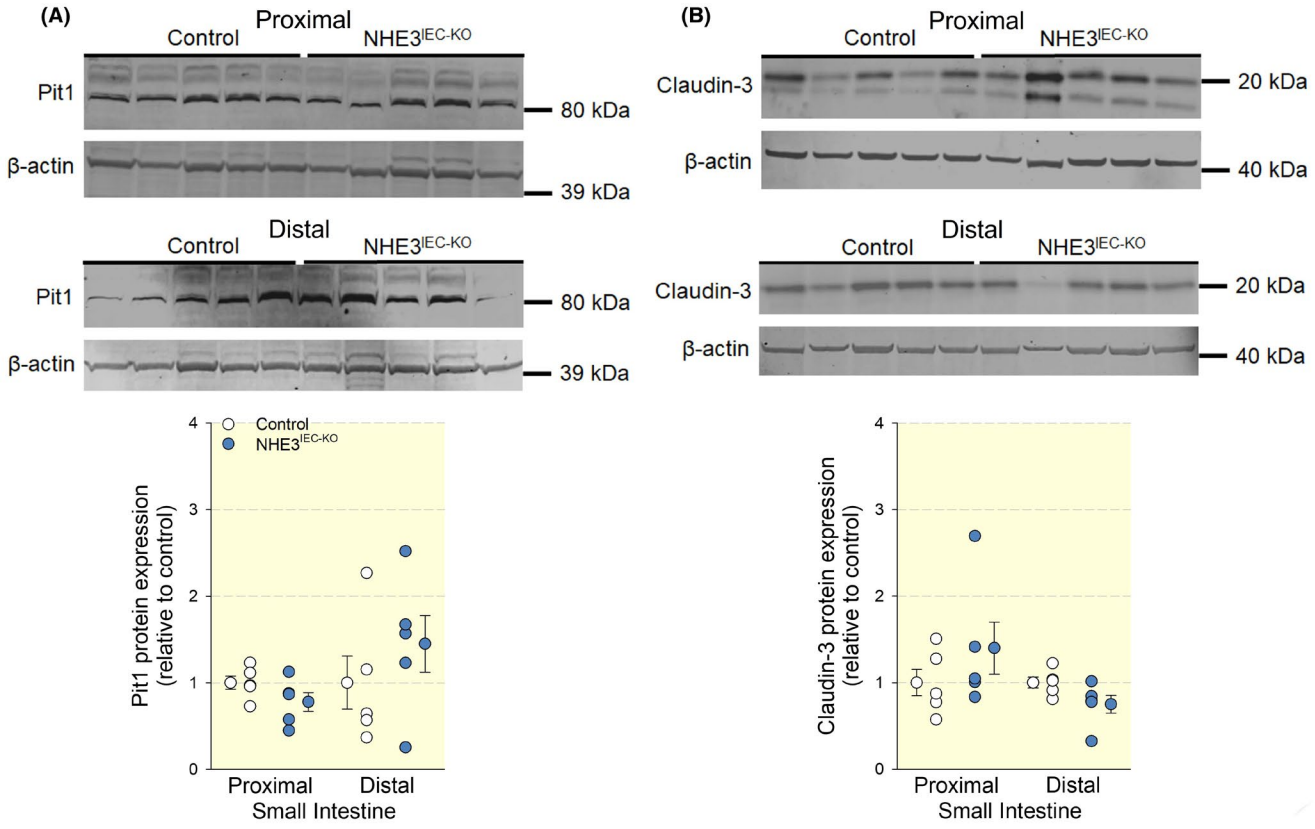


**FIGURE 7** Comparable Pit1 and claudin-3 expression between genotypes on a high $P_i$ diet. Intestinal epithelial cells were isolated 2 weeks after high dietary $P_i$ feeding. (A) Pit1 protein expression (predicted molecular weight ~82 kDa; β-actin, predicted molecular weight ~42 kDa) was not significantly different between genotypes in the proximal and distal small intestine (n = 5/genotype). (B) Claudin-3 expression (predicted molecular weight ~20 kDa) was not significantly different between genotypes in the proximal and distal small intestine (n = 5/genotype). Male mice were used in these studies. Data are expressed as mean ± SEM and were analysed by Student's *t* test

further consistent with enhanced $P_i$ absorption because of a greater Npt2b expression. NHE3$^{IEC-KO}$ mice have greater intestinal permeability associated with a ~25% reduced expression of the tight junction protein occludin.[3] However, whether or not these findings can explain increased paracellular $P_i$ uptake remains elusive. Our studies on $^{33}P$ appearance in the plasma of NHE3$^{IEC-KO}$ mice, which was less at the 5-minute time-point than in control mice, argue against such a mechanism. Claudin-3 has been implicated in paracellular $P_i$ transport[16,28] and everted gut sac experiments in claudin-3 knockout mice showed greater $P_i$ permeability.[28] In contrast, we found no differences in claudin-3 expression between genotypes.

We hypothesized that the exposure to more dietary $P_i$ would unravel a contribution of NHE3 for intestinal $P_i$ uptake, consistent with findings that the amount of dietary $P_i$ correlates inversely with the expression levels of Npt2b under normal conditions[25] and when kidney function is impaired.[29] Switching control mice to high dietary $P_i$ resulted in expected adaptive changes in their physiology: increased urinary $P_i$ excretion most likely because of elevated PTH and FGF23 levels. Of note, on the control diet, NHE3$^{IEC-KO}$ mice showed a slight reduction in FGF23 levels, a response not observed in normal rats treated with tenapanor.[9] In whole-body NHE3 knockout, mice FGF23 was never determined and PTH levels were not significantly different from wild-type mice.[30] Tenapanor treatment did result in reduced FGF23 levels in a rat model of CKD[31] and patients receiving haemodialysis with hyperphosphatemia.[12] Importantly, tenapanor combined with a $P_i$ binder had synergistic effects on plasma $P_i$ and FGF23 levels,[10,15] indicating that the inhibitory effect of tenapanor does not account for all intestinal $P_i$ uptake. If tenapanor, independent of its mode of action, would inhibit the majority of intestinal $P_i$ uptake, then $P_i$ binders should have no additional effect. In a $^{33}P$ uptake study in rats using NTX792 (a close analogue of tenapanor), the area under the curve was only reduced by ~35%,[31] suggesting the drug does not inhibit the majority of intestinal $P_i$ uptake. Our data using the same protocol indicate that the inhibitory effect of tenapanor on $^{33}P$ appearance in plasma of mice is (a) only detected 5 minutes after administration and (b) followed by a second phase with

increased absorption at 60 minutes. The latter is likely the cause for why no differences in the area under the curve were observed. The early (5-minute time-point) inhibitory effect, despite greater Npt2b expression, seems to be specific for NHE3 because no differences between vehicle and tenapanor treatment were observed in $NHE3^{IEC\text{-}KO}$ mice. However, our data showing different effects of tenapanor compared to vehicle in $NHE3^{IEC\text{-}KO}$ mice suggest the existence of possible off-target effects. After 1 week of high dietary $P_i$, plasma $P_i$ in $NHE3^{IEC\text{-}KO}$ mice was significantly greater compared with control mice and remained significantly greater after 2 weeks of high $P_i$ diet. Challenging mice by acute oral $P_i$ loading showed that plasma $P_i$ levels increased to greater levels in $NHE3^{IEC\text{-}KO}$ compared with control mice. Consistent with this enhanced $P_i$ uptake, Npt2b expression was significantly greater in $NHE3^{IEC\text{-}KO}$ mice after 2 weeks on a high $P_i$ diet.

What might explain these discrepancies in $P_i$ homeostasis between $NHE3^{IEC\text{-}KO}$ mice and tenapanor? Pharmacological inhibition of intestinal transporters is an interesting approach for the treatment of gastrointestinal or more systemic diseases. For example, mizagliflozin is a $Na^+$/glucose cotransporter 1 (Sglt1) inhibitor that was developed to treat constipation.[32] Of note, Sglt1 knockout mice show a 100% mortality rate after weaning because of severe osmotic diarrhoea.[33] In conjunction with our data in intestinal-specific NHE3 knockout compared to tenapanor, genetic deletion seems to have a stronger/more detrimental effect, even when induced in adulthood, compared to pharmacological inhibition. NHE3 knockout could have secondary consequences on interacting proteins/protein complexes, which is less likely expected from pharmacological inhibition. Several other possibilities exist, including but not limited to: (a) species differences,[22,23,34] (b) existence of other $P_i$ transporters[24,35] and/or (c) importance of paracellular $P_i$ uptake[9,36]; the latter 2 could be targeted directly and/or indirectly by tenapanor. However, the lack of Npt2b has not been described to upregulate the paracellular $P_i$ absorption pathway.[36] Of note, 1 study showed that in CKD, Npt2b might not be an ideal target to improve $P_i$ homeostasis, as the Npt2b inhibitor ASP3325 did not affect hyperphosphatemia in patients with end-stage renal disease undergoing haemodialysis.[37] Remarkably, a novel pan-phosphate transporter inhibitor (EOS789, Npt2a, Pit1/2) was able to maintain lower levels of plasma $P_i$ in parallel with FGF23 and PTH in a long-term study[38] and was found to be safe in a phase 1b clinical trial in haemodialysis patients.[39]

Tenapanor is proposed to be used to treat hyperphosphatemia in CKD, a condition where intestinal Npt2b is downregulated.[35] Of note, tenapanor treatment in healthy rats does not affect plasma $P_i$, PTH, FGF23 or 25-OH vitamin D levels,[9] effects that were present in a rat model of CKD[31] and patients on hemodialysis.[10-12] A recent study identified major differences in intestinal $P_i$ transport between normal rats and rats with CKD and proposed the possible existence of a yet unknown $P_i$ transporter.[35] If this transporter is identical to a PFA-inhabitable $Na^+$-dependent $P_i$ transporter,[24] and if this transporter is a target of tenapanor, remains to be determined.

In summary, we hypothesized that intestinal-specific NHE3 knockout would mimic pharmacological inhibition of NHE3 and show other features of reduced intestinal $P_i$ uptake. In contrast, $NHE3^{IEC\text{-}KO}$ mice show a phenotype of Npt2b overexpression and enhanced $P_i$ absorption. More studies are needed to better understand the differences in $P_i$ transport between tenapanor and $NHE3^{IEC\text{-}KO}$ mice and overall $P_i$ handling by the intestine.

## 4 | MATERIALS AND METHODS

All the material submitted is conformed with good publishing practise in physiology.[40]

### 4.1 | Animals and diets

All animal experimentation was conducted in accordance with the Guide for Care and Use of Laboratory Animals (National Institute of Health) and was approved by the University of South Florida Institutional Animal Care and Use Committee (3338R and 7525R). Floxed NHE3 ($NHE3^{loxlox}$) female mice were crossed with male $NHE3^{IEC\text{-}KO}$ mice.[3] Mice were on an albino C57BL/6J background and genotyped by a polymerase chain reaction from genomic DNA isolated from ear punch. Genotyping for the floxed allele and Cre were previously described.[3] Mice were housed under a 12:12-hour light-dark cycle in isolated ventilated cages with free access to standard (control, 0.4% as non-phytate phosphorus) rodent chow (TD.2018; Envigo, Madison, WI) and tap water. Littermate age-matched, 3- to 6-month-old mice (control, $NHE3^{loxlox}$) or $NHE3^{IEC\text{-}KO}$ mice were used for experiments. Male mice were used, except where indicated in the figure legends. NHE3 deletion was induced using tamoxifen (67 mg $kg^{-1}$), initially dissolved in 5% (v/v) of ethanol followed by adding 95% (v/v) of corn oil. Tamoxifen was administered via oral gavage (volume 1% of body weight) for 5 consecutive days to control and $NHE3^{IEC\text{-}KO}$ mice. High dietary $P_i$ manipulations were performed by feeding mice a 1.5% $P_i$ diet (TD.140038, Envigo).[41] All acute experiments (blood collections, tissue harvesting, oral $P_i$ loading) were performed between 9:00 and 12:00 PM. A

consort flow chart depicting the performed studies is provided as Figure S2.

## 4.2 | Physiological analysis

Body weight, fluid and food intake were determined daily after tamoxifen induction for up to 10 days and averaged. Blood was collected before and 14 days after induction as well as after 14 days on high dietary $P_i$ under brief isoflurane anaesthesia from the retro-orbital plexus. Spontaneously voided urine was collected daily by reflex urination holding mice over a clean petri dish in combination with gentle bladder expression if needed. Values from multiple days were averaged.

## 4.3 | Analysis of intestinal content

Mice on a control diet were euthanized 2 weeks after tamoxifen administration via isoflurane overdose. In another cohort, mice were administered tamoxifen, fed a control diet for 2 weeks, followed by an additional 2 weeks of high $P_i$ diet and were then euthanized. After euthanasia, the small intestine and colon were removed. The small intestine was cut into 2 segments of equal length, labelled with proximal (closest to the stomach) and distal, respectively. Subsequently, the contents of the proximal and distal segments as well as of the colon were extruded into 5 mL tubes. The weight of the content was determined gravimetrically and 0.75 mol $L^{-1}$ $HNO_3$ was added equal to 5-fold the weight of the contents. Then, the samples were homogenized by ultrasonication (Sonic Dismembrator Model F60, Fisher Scientific). After overnight incubation at room temperature, samples were centrifuged at 1,000*g* for 5 minutes to pellet debris. Then the supernatants were transferred into 1.5 mL tubes for centrifugation at 17,000*g* for 20 minutes. After centrifugation, the final supernatants were collected and analysed for $Na^+$ and $P_i$, as described below.

## 4.4 | Acute hyperphosphatemic model

Two weeks after tamoxifen administration, mice on the control diet were gavaged with vehicle (sterile water, 1% of body weight) or a 0.5 mol $L^{-1}$ $NaH_2PO_4$ solution.[42] In another set of mice, the same experiment was performed after mice were fed for 1 week a high $P_i$ diet. Blood was collected before gavage and 60 minutes after administration. Plasma $P_i$ was measured as described below.

## 4.5 | Effect of tenapanor on intestinal $^{33}P$ uptake

Uptake studies of $^{33}P$ (ARP 0133, American Radiolabeled Chemicals, Inc) were performed in a separate cohort of mice on the control diet 2 weeks after tamoxifen administration. To study the acute effect of tenapanor on $P_i$ absorption, the appearance of $^{33}P$ in plasma was determined in control and $NHE3^{IEC\text{-}KO}$ mice. After overnight fasting,[31] mice were gavaged (volume: 1% of body weight) with vehicle (5% DMSO, 5% Cremophor EL, 90% a solution of 50 μCi $mL^{-1}$ $^{33}P$, 8 mmol $L^{-1}$ $NaH_2PO_4$ and 4 mmol $L^{-1}$ $CaCl_2$) or tenapanor (30 mg $kg^{-1}$ in vehicle, Cayman Chemical Company). Blood was collected before gavage, and at 5, 30, 60 and 120 minutes after gavage under brief isoflurane anaesthesia. After centrifugation, plasma was transferred into scintillation vials containing 3 mL of scintillation cocktail (Liquiscint, National Diagnostics) before radioactivity was measured in a LS 6500 scintillation counter (Beckman Coulter).

## 4.6 | Everted gut sac experiments

Two weeks after tamoxifen administration, mice on a control diet were euthanized via isoflurane overdose and the small intestine removed. After flushing with isotonic saline, a 5-cm duodenal segment distal of the pyloric sphincter was removed, for the ileum, a 5-cm segment proximal of the caecum was removed and, for the jejunum, a 5-cm segment in the middle of the remainder of the intestine was removed. Subsequently, segments were inverted using a blunt-ended metal rod. One end of the segment was ligated with a braided silk suture (4-0) and the serosal side was filled with 400 μL of transport buffer (in mmol $L^{-1}$: NaCl/choline $Cl^-$, 140; KCl, 5; $MgCl_2$, 1; $CaCl_2$, 2; HEPES-Tris, 10 (pH 7.4); $KH_2PO_4$, 1; glucose, 5; gassed with 95% $O_2$/5% $CO_2$, at 37°C) using a blunt end needle ($Na^+$-free conditions were studied by replacing NaCl with choline $Cl^-$). The needle was removed, the other end ligated, and the segment weighed. The segments were placed for 1 hour in jacketed beakers, prefilled with 40 mL of transport buffer and connected to a circulating water bath which maintained the temperature at 37°C. The transport buffer containing the segments was aerated continuously with 95% $O_2$/5% $CO_2$. After 1 hour the sacs were removed, gently blotted dry and weighed. Subsequently, the sacs were cut open and the fluid from each sac, as well as the transport buffer, were assayed for $P_i$ and glucose as described below.

### 4.7 | Intestinal brush border membrane vesicles (BBMV)

Epithelial cells for the preparation of BBMV were prepared by $Ca^{2+}$ chelation[3,43] followed by the $Mg^{2+}$ precipitation technique.[44,45] Briefly, female mice on a control diet for 2 weeks after tamoxifen administration were euthanized by isoflurane overdose. The small intestine was flushed and separated into duodenum, jejunum and ileum. Subsequently, the intestinal segments were everted; one end was ligated, and the everted segments were filled with $Ca^{2+}$-free PBS containing 5 mmol $L^{-1}$ ethylenediaminetetraacetic acid (EDTA), pH 7.4. The everted pieces were put in 50 mL tubes containing 40 mL $Ca^{2+}$-free PBS+EDTA and incubated in a water bath at 37∘C for 20 minutes. Every 5 minutes, the tubes were vigorously shaken to release the epithelial cells. After the removal of sacs devoid of epithelial cells, the solution was centrifuged. For each segment, the cells isolated from 2 mice were combined. Cells were homogenized in buffer containing (in mmol $L^{-1}$): mannitol, 50; HEPES-NaOH, 2; pH 7.1, supplemented with protease inhibitor (Pierce™, Thermo Fisher Scientific). BBMVs, after being isolated by the $Mg^{2+}$-precipitation technique,[46] were resuspended in buffer containing 300 mmol $L^{-1}$ mannitol and 16 mmol $L^{-1}$ Tris-HEPES, pH 7.5. Uptake of $^{32}P$ into BBMVs was performed according to the rapid filtration technique.[47] Briefly,10 μL freshly prepared BBMVs were incubated at room temperature for 30 seconds in a 40-μL uptake medium containing 150 mmol $L^{-1}$ NaCl, 16 mmol $L^{-1}$ Tris-HEPES, pH 6 (for duodenum or jejunum) or pH 7.4 (for ileum). In addition, the uptake solution contained 0.1 mmol $L^{-1}$ $K_2HPO_4/KH_2PO_4$ (pH 7.4) as cold substrate and $^{32}P$ (10 μCi $mL^{-1}$) as a tracer. NaCl was replaced with choline $Cl^-$ to determine $Na^+$ independent uptake, and 30 mmol $L^{-1}$ phosphonoformic acid (PFA) was added to the $Na^+$ uptake solution to study PFA (Npt2b)-mediated uptake. After the incubation, uptake was stopped by adding 1-mL ice-cold stop solution (100 mmol $L^{-1}$ choline $Cl^-$, 100 mmol $L^{-1}$ mannitol, 5 mmol $L^{-1}$ HEPES-Tris, pH 7.5). The vortexed suspensions were pipetted onto 0.45 μm mixed cellulose ester membranes (MilliporeSigma) that were immediately vacuum washed with 15 mL of ice-cold stop solution. Membranes were transferred into scintillation vials containing 3 mL of scintillation cocktail (Liquiscint) before radioactivity was measured in a β-counter. The protein concentrations of BBMVs were determined using a Bio-Rad DC Protein assay (Bio-Rad Laboratories). Uptake for each condition/segment was performed in triplicate except for choline $Cl^-$ experiments which were performed in duplicate. All experiments were repeated 4 times/genotype.

### 4.8 | Analysis of urine, plasma, everted gut sac samples and intestinal contents

Blood chemistry was determined by an OPTI® CCA-TS2 blood gas analyser using an E-Cl Type cassette (OPTIMedical). Blood, urine, gut sac and intestinal content clinical chemistry were performed using commercially available assays that were modified to work with small volumes.[48,49] The concentration of hormones was determined using the following commercially available assays: PTH (1-84; Quidel Corporation), intact FGF-23 (Quidel Corporation). Urinary creatinine was determined using Infinity™ Creatinine Liquid Stable Reagent (Thermo Fisher Scientific). Glucose and $P_i$ concentrations were determined using commercially available assays (Thermo Fisher Scientific Glucose Hexokinase Reagent and Pointe Scientific Phosphorus Reagent, respectively). $Na^+$ was measured by flame photometry (BWB Technologies Ltd.).

### 4.9 | Immunoblot analysis

Isolated intestinal epithelial cells were homogenized in buffer (250 mmol $L^{-1}$ sucrose, 10 mmol $L^{-1}$ triethanolamine, Sigma-Aldrich) containing protease and phosphatase inhibitors (both from Fisher Scientific). The homogenate was centrifuged at 1000*g* for 15 minutes, and the resultant supernatant was further centrifuged at 17,000*g* for 30 minutes. Pellets were resuspended and used for western blotting. Equal lane loading (20 μg for intestine) was achieved using a Bio-Rad DC Protein assay (Bio-Rad Laboratories). Samples were resolved on NuPAGE 4%-12% or 12% Bis-Tris gels in MOPS. Gel proteins were transferred to PVDF membranes and immunoblotted with antibodies against Npt2a (dilution 1:1,500, rabbit, gift from M Levi[50]), Npt2b (dilution 1:1,500, rabbit, gift from M Levi[50]), Npt2c (dilution 1:1,500, rabbit, gift from M Levi[50]), claudin-3 (dilution 1:1,000, rabbit, catalogue # 34-1700, Thermo Fisher Scientific), Pit1 (dilution 1:500, rabbit, gift from V Sorribas[24]) and β-actin (dilution 1:30,000, mouse, Sigma-Aldrich). Detection was performed with secondary antibodies against rabbit (IRDye® 800CW donkey anti-rabbit IgG, dilution 1:5,000) or mouse (IRDye® 680RD donkey anti-mouse IgG, dilution 1:5,000) and detected with an Odyssey® CLx (LI-COR Biosciences). Densitometric analysis was performed using Image Studio Lite (LI-COR Biosciences).

### 4.10 | Statistical analyses

Data are expressed as mean ± SEM Unpaired Student's *t* test was performed to analyse statistical differences

between groups. One-way analysis of variance (ANOVA), two-way mixed-effects model or ANOVA followed by a two-stage linear step-up procedure of Benjamini, Krieger and Yekutieli, Šidák or Tukey's multiple comparison tests, as indicated, were used to test for significant differences between genotype or experimental conditions. All data were analysed via GraphPad Prism Version 8.3 or SigmaPlot Version 12.5). Significance was considered at $P < .05$.

## ACKNOWLEDGEMENTS

The antibody for Pit1 was kindly provided by Victor Sorribas, (University of Zaragoza, Spain). This work was supported by the National Institute of Diabetes and Digestive and Kidney Diseases grant 1R01DK110621 (to Dr Rieg), VA Merit Review Award IBX004968A (to Dr Rieg) and an American Heart Association Transformational Research Award 19TPA34850116 (to Dr Rieg). Financial support for this work was also provided by the NIDDK Diabetic Complications Consortium (RRID:SCR_001415, www.diacomp.org), grants DK076169 and DK115255 (to Dr Rieg). Dr Thomas was supported by an American Heart Association postdoctoral fellowship (19POST34400026 and 828731) and Dr Xue by a predoctoral fellowship (18PRE33990236). Further funding to Dr Fenton was provided by the Novo Nordisk Foundation (NNF17OC0028812 and NNF19OC0058439) and the Danish Council for Independent Research (0134-00018B).

## CONFLICT OF INTEREST

TR had a consultancy agreement with Ardelyx. The other authors declare that they have no competing financial interests.

## AUTHOR CONTRIBUTIONS

Dr Rieg conceived and designed the work. Dr Thomas, Dr Xue, Dr Dominguez Rieg, Dr Fenton, Dr Murali and Dr Rieg contributed to the acquisition, analysis, or interpretation of data for the work. Dr Levi provided reagent. Dr Rieg drafted the work; Dr Thomas, Dr Xue, Dr Levi, Dr Fenton, Dr Murali and Dr Dominguez Rieg revised it critically for important intellectual content. Dr Thomas, Dr Xue, Dr Levi, Dr Fenton, Dr Murali, Dr Dominguez Rieg and Dr Rieg approved the final version of the manuscript.

## DATA AVAILABILITY STATEMENT

The data that support the findings of this study are available from the corresponding author upon reasonable request.

## ORCID

*Timo Rieg* https://orcid.org/0000-0001-6082-662X

## REFERENCES

1. Fenton RA, Poulsen SB, de la Mora CS, Soleimani M, Dominguez Rieg JA, Rieg T. Renal tubular NHE3 is required in the maintenance of water and sodium chloride homeostasis. *Kidney Int*. 2017;92(2):397-414.
2. Schultheis PJ, Clarke LL, Meneton P, et al. Renal and intestinal absorptive defects in mice lacking the NHE3 Na+/H+ exchanger. *Nat Genet*. 1998;19(3):282-285.
3. Xue J, Thomas L, Tahmasbi M, et al. An inducible intestinal epithelial cell-specific NHE3 knockout mouse model mimicking congenital sodium diarrhea. *Clin Sci (Lond)*. 2020;134(8):941-953.
4. Dimitrov G, Bamberger S, Navard C, et al. Congenital sodium diarrhea by mutation of the SLC9A3 gene. *Eur J Med Genet*. 2019;62(10):103712.
5. Gawenis LR, Stien X, Shull GE, et al. Intestinal NaCl transport in NHE2 and NHE3 knockout mice. *Am J Physiol Gastrointest Liver Physiol*. 2002;282(5):G776-G784.
6. Zielinska M, Wasilewski A, Fichna J. Tenapanor hydrochloride for the treatment of constipation-predominant irritable bowel syndrome. *Expert Opin Investig Drugs*. 2015;24(8):1093-1099.
7. Spencer AG, Labonte ED, Rosenbaum DP, et al. Intestinal inhibition of the Na+/H+ exchanger 3 prevents cardiorenal damage in rats and inhibits Na+ uptake in humans. *Sci Transl Med*. 2014;6(227):227ra236.
8. Johansson S, Rosenbaum DP, Knutsson M, Leonsson-Zachrisson M. A phase 1 study of the safety, tolerability, pharmacodynamics, and pharmacokinetics of tenapanor in healthy Japanese volunteers. *Clin Exp Nephrol*. 2017;21(3):407-416.
9. King AJ, Siegel M, He Y, et al. Inhibition of sodium/hydrogen exchanger 3 in the gastrointestinal tract by tenapanor reduces paracellular phosphate permeability. *Sci Transl Med*. 2018;10(456):aam6474
10. Pergola PE, Rosenbaum DP, Yang Y, Chertow GM. A randomized trial of tenapanor and phosphate binders as a dual-mechanism treatment for hyperphosphatemia in patients on maintenance dialysis (AMPLIFY). *J Am Soc Nephrol*. 2021;32(6):1465-1473.
11. Block GA, Rosenbaum DP, Yan A, Chertow GM. Efficacy and safety of tenapanor in patients with hyperphosphatemia receiving maintenance hemodialysis: a randomized phase 3 trial. *J Am Soc Nephrol*. 2019;30(4):641-652.
12. Block GA, Rosenbaum DP, Yan A, Greasley PJ, Chertow GM, Wolf M. The effects of tenapanor on serum fibroblast growth factor 23 in patients receiving hemodialysis with hyperphosphatemia. *Nephrol Dial Transplant*. 2019;34(2):339-346.
13. Faul C, Amaral AP, Oskouei B, et al. FGF23 induces left ventricular hypertrophy. *J Clin Invest*. 2011;121(11):4393-4408.
14. Ardelyx, Inc. July 2021. https://ir.ardelyx.com/news-releases/news-release-details/ardelyx-receives-complete-response-letter-us-fda-new-drug. Accessed October 18, 2021.
15. King AJ, Kohler J, Fung C, et al. Combination treatment with tenapanor and sevelamer synergistically reduces urinary phosphorus excretion in rats. *Am J Physiol Renal Physiol*. 2021;320(1):F133-F144.
16. Tanaka H, Imasato M, Yamazaki Y, et al. Claudin-3 regulates bile canalicular paracellular barrier and cholesterol gallstone core formation in mice. *J Hepatol*. 2018;69(6):1308-1316.
17. Wang JL, Zhao L, Zhu J, et al. Expression, Localization, and Effect of High Salt Intake on Electroneutral Na(+)/HCO3 (-)

Cotransporter NBCn2 in Rat Small Intestine: Implication in Intestinal NaCl Absorption. *Front Physiol*. 2019;10:1334.
18. U.S. Food and Drug Administration. Full prescribing information, September 2019. https://www.accessdata.fda.gov/drugsatfda_docs/label/2019/211801s000lbl.pdf. Accessed October 18, 2021.
19. Marks J, Lee GJ, Nadaraja SP, Debnam ES, Unwin RJ. Experimental and regional variations in Na+-dependent and Na+-independent phosphate transport along the rat small intestine and colon. *Physiol Rep*. 2015;3(1):e12281.
20. Hu MS, Kayne LH, Jamgotchian N, Ward HJ, Lee DB. Paracellular phosphate absorption in rat colon: a mechanism for enema-induced hyperphosphatemia. *Miner Electrolyte Metab*. 1997;23(1):7-12.
21. Radanovic T, Wagner CA, Murer H, Biber J. Regulation of intestinal phosphate transport. I. Segmental expression and adaptation to low-P(i) diet of the type IIb Na(+)-P(i) cotransporter in mouse small intestine. *Am J Physiol Gastrointest Liver Physiol*. 2005;288(3):G496-G500.
22. Marks J, Srai SK, Biber J, Murer H, Unwin RJ, Debnam ES. Intestinal phosphate absorption and the effect of vitamin D: a comparison of rats with mice. *Exp Physiol*. 2006;91(3):531-537.
23. Walton J, Gray TK. Absorption of inorganic phosphate in the human small intestine. *Clin Sci (Lond)*. 1979;56(5):407-412.
24. Candeal E, Caldas YA, Guillen N, Levi M, Sorribas V. Intestinal phosphate absorption is mediated by multiple transport systems in rats. *Am J Physiol Gastrointest Liver Physiol*. 2017;312(4):G355-G366.
25. Giral H, Caldas Y, Sutherland E, et al. Regulation of rat intestinal Na-dependent phosphate transporters by dietary phosphate. *Am J Physiol Renal Physiol*. 2009;297(5):F1466-F1475.
26. Madunic IV, Breljak D, Karaica D, Koepsell H, Sabolic I. Expression profiling and immunolocalization of Na(+)-D-glucose-cotransporter 1 in mice employing knockout mice as specificity control indicate novel locations and differences between mice and rats. *Pflugers Arch*. 2017;469(12):1545-1565.
27. Sabbagh Y, O'Brien SP, Song W, et al. Intestinal npt2b plays a major role in phosphate absorption and homeostasis. *J Am Soc Nephrol*. 2009;20(11):2348-2358.
28. Hashimoto N, Matsui I, Ishizuka S, et al. Lithocholic acid increases intestinal phosphate and calcium absorption in a vitamin D receptor dependent but transcellular pathway independent manner. *Kidney Int*. 2020;97(6):1164-1180.
29. Aniteli TM, de Siqueira FR, Dos Reis LM, et al. Effect of variations in dietary Pi intake on intestinal Pi transporters (NaPi-IIb, PiT-1, and PiT-2) and phosphate-regulating factors (PTH, FGF-23, and MEPE). *Pflugers Arch*. 2018;470(4):623-632.
30. Pan W, Borovac J, Spicer Z, et al. The epithelial sodium/proton exchanger, NHE3, is necessary for renal and intestinal calcium (re)absorption. *Am J Physiol Renal Physiol*. 2012;302(8):F943-F956.
31. Labonte ED, Carreras CW, Leadbetter MR, et al. Gastrointestinal inhibition of sodium-hydrogen exchanger 3 reduces phosphorus absorption and protects against vascular calcification in CKD. *J Am Soc Nephrol*. 2015;26(5):1138-1149.
32. Fukudo S, Endo Y, Hongo M, et al. Safety and efficacy of the sodium-glucose cotransporter 1 inhibitor mizagliflozin for functional constipation: a randomised, placebo-controlled, double-blind phase 2 trial. *Lancet Gastroenterol Hepatol*. 2018;3(9):603-613.
33. Gorboulev V, Schurmann A, Vallon V, et al. Na(+)-D-glucose cotransporter SGLT1 is pivotal for intestinal glucose absorption and glucose-dependent incretin secretion. *Diabetes*. 2012;61(1):187-196.
34. Ichida Y, Hosokawa N, Takemoto R, et al. Significant species differences in intestinal phosphate absorption between dogs, rats, and monkeys. *J Nutr Sci Vitaminol (Tokyo)*. 2020;66(1):60-67.
35. Ichida Y, Ohtomo S, Yamamoto T, et al. Evidence of an intestinal phosphate transporter alternative to type IIb sodium-dependent phosphate transporter in rats with chronic kidney disease. *Nephrol Dial Transplant*. 2021;36(1):68-75.
36. Knopfel T, Himmerkus N, Gunzel D, Bleich M, Hernando N, Wagner CA. Paracellular transport of phosphate along the intestine. *Am J Physiol Gastrointest Liver Physiol*. 2019;317(2):G233-G241.
37. Larsson TE, Kameoka C, Nakajo I, et al. NPT-IIb inhibition does not improve hyperphosphatemia in CKD. *Kidney Int Rep*. 2018;3(1):73-80.
38. Tsuboi Y, Ohtomo S, Ichida Y, et al. EOS789, a novel pan-phosphate transporter inhibitor, is effective for the treatment of chronic kidney disease-mineral bone disorder. *Kidney Int*. 2020;98(2):343-354.
39. Hill Gallant KM, Stremke ER, Trevino LL, et al. EOS789, a broad-spectrum inhibitor of phosphate transport, is safe with an indication of efficacy in a phase 1b randomized crossover trial in hemodialysis patients. *Kidney Int*. 2021;99(5):1225-1233.
40. Persson PB. Good publication practice in physiology 2019. *Acta Physiol (Oxf)*. 2019;227(4):e13405.
41. Thomas L, Xue J, Dominguez Rieg JA, Rieg T. Contribution of NHE3 and dietary phosphate to lithium pharmacokinetics. *Eur J Pharm Sci*. 2019;128:1-7.
42. Fenton RA, Murray F, Dominguez Rieg JA, Tang T, Levi M, Rieg T. Renal phosphate wasting in the absence of adenylyl cyclase 6. *J Am Soc Nephrol*. 2014;25(12):2822-2834.
43. Fenton RA, Murali SK, Kaji I, et al. Adenylyl cyclase 6 expression is essential for cholera toxin-induced diarrhea. *J Infect Dis*. 2019;220(11):1719-1728.
44. Hernando N, Myakala K, Simona F, et al. Intestinal depletion of NaPi-IIb/Slc34a2 in mice: renal and hormonal adaptation. *J Bone Miner Res*. 2015;30(10):1925-1937.
45. Layunta E, Pastor Arroyo EM, Kagi L, et al. Intestinal response to acute intragastric and intravenous administration of phosphate in rats. *Cell Physiol Biochem*. 2019;52(4):838-849.
46. Biber J, Stieger B, Stange G, Murer H. Isolation of renal proximal tubular brush-border membranes. *Nat Protoc*. 2007;2(6):1356-1359.
47. Stoll R, Kinne R, Murer H. Effect of dietary phosphate intake on phosphate transport by isolated rat renal brush-border vesicles. *Biochem J*. 1979;180(3):465-470.
48. Thomas L, Xue J, Tomilin VN, Pochynyuk OM, Dominguez Rieg JA, Rieg T. PF-06869206 is a selective inhibitor of renal Pi transport: evidence from in vitro and in vivo studies. *Am J Physiol Renal Physiol*. 2020;319(3):F541-F551.
49. Thomas L, Xue J, Murali SK, Fenton RA, Dominguez Rieg JA, Rieg T. Pharmacological Npt2a inhibition causes phosphaturia and reduces plasma phosphate in mice with normal and reduced kidney function. *J Am Soc Nephrol*. 2019;30(11):2128-2139.

50. Caldas YA, Giral H, Cortazar MA, et al. Liver X receptor-activating ligands modulate renal and intestinal sodium-phosphate transporters. *Kidney Int*. 2011;80(5):535-544.

## SUPPORTING INFORMATION

Additional supporting information may be found in the online version of the article at the publisher's website.

**How to cite this article:** Xue J, Thomas L, Murali SK, et al. Enhanced phosphate absorption in intestinal epithelial cell-specific NHE3 knockout mice. *Acta Physiol*. 2022;234:e13756. doi:10.1111/apha.13756